# Considerations on the equivalent electric models of a UHF RFID Helical Antenna Yarn

Sofia Benouakta, Santasri Koley, Florin Hutu, Yvan Duroc

# Considerations on the equivalent electric models of a UHF RFID Helical Antenna Yarn

Sofia Benouakta*, Santasri Koley*, Florin Hutu† and Yvan Duroc*
*Université de Lyon, Université Claude Bernard Lyon1, CNRS, Ampère, F-69622, Villeurbanne, France
†Univ Lyon, INSA Lyon, Inria, CITI, F-69621, Villeurbanne, France
Email: florin-doru.hutu@insa-lyon.fr

***Abstract*— The aim of this paper is to present different ways to extract electrical models of an antenna specifically designed for Radio Frequency IDentification (RFID) Ultra High Frequency (UHF) communications. More precisely the models are extracted from a helical dipole designed to operate in the European RFID band and in the context of smart textiles. This kind of antenna was chosen because its electrical properties and radiation pattern are relatively robust with respect of stretching deformation. After presenting the antenna's design, two strategies to extract antenna models are discussed and then compared. The first method is taking into account the antenna's physical dimensions and shape, and the second one, which is a general method relevant to any other antenna geometry, is based on the rational approximation of the antenna's frequency response.**

## I. Introduction

With the emergence of the Internet of Things (IoT) paradigm, where any object will be connected to data Web services, the market of wireless technologies is going to greatly increase yet more [1]. All current "low-power" communication protocols, as for instance Bluetooth Low Energy, Zigbee, Z-Wave, Sigfox or Lora, are potential candidates and also concurrent according to the needs, in terms of notably data rate and communication range.

Indeed these technologies aim to reduce the energy payload of the radio communication part to few millijoules [2], [3]. However when the application requires data rates of some hundreds kilobytes per second and the communication range is few meters, the RFID technology can present decisive advantages. Besides the inherent identification functionality, passive RFID systems rely on non-symmetric communicating nodes: the reader provides the energy to the tag and collects its information; the tag exploits the transmitted RF energy by the reader for powering its active circuits (activation) and for transmitting its data by load modulation (i.e., backscattering modulation).

Consequently, the tags that are attached to the objects do not require any embedded energy source. As the number of objects is practically infinite, it implies that the passive RFID approaches drastically eliminate the fundamental issues of battery supply in terms of maintenance and recycling, but also in terms of dimensions and weight. The RFID technology is also strongly evolving with new types of tags, so-called augmented tags, including new capabilities as sensing and actuation [4]. This fact is an advantage for the RFID in the context of the IoT where the objects will be wirelessly connected but also endowed to sense and/or act on their environment.

Otherwise, a tag is constituted by two main parts: the chip and the antenna. The manufacturers propose new chips with always improved performance in terms of sensitivity (i.e., indirectly in terms of read range) or currently integrating new capabilities. Furthermore, for RFID tags designers, it is well known that the antenna is the most critical part [5]. Indeed, the antenna design has to take into consideration as well as the future attached object and the associated chip. Classically, the input impedance antenna will be matched to 50 $\Omega$ impedance. In the case of RFID, the reference is the chip impedance(s), i.e., the matched impedance for activation improvement or modulation impedance for optimizing the delta radar cross section [6].

In order to perform the radio front-end optimization, an equivalent electrical model of the antenna's input impedance can be very useful for circuit simulations. Indeed, nowadays, electromagnetic field-circuit co-simulation is made possible by the most known simulation frameworks but this kind of approach is often time consuming and has a high computational cost. This is why, having a lumped elements equivalent electrical circuit of the antenna's input impedance is particularly important for designing optimal tags. Such electrical model could enable to design more quickly the antenna conjointly to the associated chip.

In this paper, the attention is focused on the obtaining of an equivalent electrical circuit for a helical dipole antenna operating in the European RFID band (865.5 - 867.5 MHz) and dedicated to RFID yarn design. Replacing the simple slender dipole antenna proposed in [7] for RFID E-threads by a helical antenna could enable to have a certain stretching robustness. However, the geometry of helical antennas is much more complex than a simple dipole and requires longer time for electromagnetic simulation. That is why the main objective of this paper is to present two model extraction strategies. They are based on the exploitation of the simulated (or measured) reflection coefficient and a specific electric circuit topology. The first approach is an empirical method dedicated to helical antenna and the second one is analytical and valuable for any antenna geometry.

Section II summarizes the design of the helical antenna highlighting the methodological approach and the interest in regard of the stretching. Section III details and compares the

two approaches for extracting a model for the helical antenna's input impedance. Finally, conclusion and perspectives are given in section IV.

## II. Design of the Helical Antenna Dedicated to UHF RFID Yarn

The antenna is designed to be integrated into clothes in order to bring them smart functionality as identification, sensing, etc. Consequently, the antenna should have good mechanical properties in order to assure robustness in terms of stretching. Besides, the antenna is firstly dedicated to a textile yarn implying a linear form factor. One of the shapes that is the most appropriate is the helical antenna that may surround the textile wires [8]. The helical antenna's geometry is presented in Fig. 1.

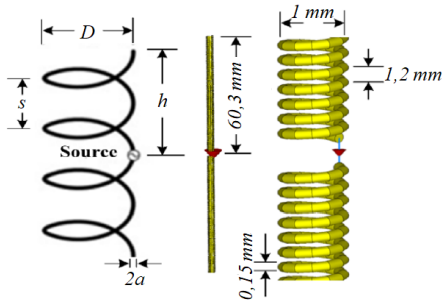


Fig. 1. Illustration of the simulated helical antenna. Left part: the main design parameters, middle: full view in CST and right part: the zoomed view around the feeding point.

The design methodology is inspired from [8]. For this study, and without loss of generality for the stretching robustness study and for the modeling part (section III), the antenna is considered in free space and the impedance matching is chosen arbitrarily close to 50 Ω. A specific material around the antenna will require the consideration of the dielectric's relative permittivity in the simulation environment, and any associated RFID chip will imply a specific impedance matching. The fundamental for the design guidelines is to worth noting how the geometrical parameters impact the antenna properties. The spacing between two adjacent turns has a strong influence on the antenna's input impedance while the antenna's length and the number of turns influence rather its resonance frequency. The antenna has been designed with CST Microwave Studio® and has the parameters given in Table I.

TABLE I

Physical Dimensions of the Proposed Antenna

| Helical diameter (D) [mm] | Number of turns N | Spacing between turns (s) [mm] | Wire diameter (a) [mm] | Antenna's half length (h) [mm] |
|---|---|---|---|---|
| 1 | 50.5 | 1.2 | 0.15 | 60.3 |

The resonance frequency is 868 MHz and, at this specific frequency, the input impedance $Z_{ant} = 40.33 + j \cdot 4.26\ \Omega$, which corresponds to a reflection coefficient $S_{11} = -19\ dB$. The reflection coefficient is defined as:

$$S_{11} = 20 \log_{10} \left( \frac{Z_{ant} - Z_{ref}}{Z_{ant} + Z_{ref}} \right) \quad (1)$$

where $Z_{ref}$ is the reference impedance.

In order to evaluate the robustness of the antenna against stretching, parametric simulations have been performed when the length of the helical antenna is extended from the initial length ($h_0$ = 60.3 mm) up to 66.3 mm while keeping the same number of turns.

For each length, the relative elongation defined as:

$$E\ [\%] = \frac{h - h_0}{h_0} \cdot 100 \quad (2)$$

was calculated and Table II presents the considered relative elongations together to the antenna's resonance frequency.

TABLE II

Relative Elongation for Each Considered Length

| h [mm] | 60.3 | 62.3 | 64.3 | 66.3 |
|---|---|---|---|---|
| E [%] | 0 | 3.3 | 6.6 | 9.9 |
| f [MHz] | 868 | 848.1 | 829.2 | 813 |

Fig. 2 shows the associated reflection coefficients. As can be remarked, the resonance frequency is shifted to the lower frequencies when the elongation increases (i. e., when the antenna is stretched). Moreover, the reflection coefficient $S_{11}$ decreases when stretching deformation increases. For an elongation until 4%, the bandwidth defined at $-10$ dB is still sufficient for ensuring the RFID communication link. The radiation pattern for a helical antenna is similar than a dipole antenna with a gain loss of 3 dB. The elongation will not impact the radiation pattern.

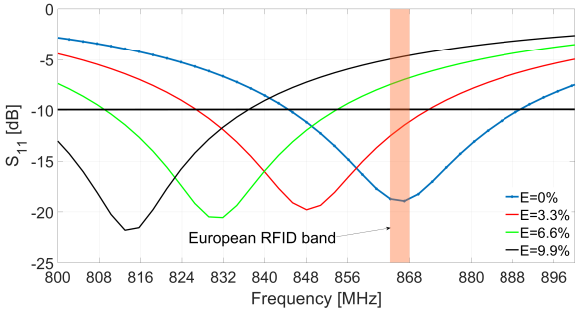


Fig. 2. Impact of the elongation on the resonance frequency and on the reflection coefficient $S_{11}$.

## III. Equivalent Circuit Extraction of the Antenna's Input Impedance

### A. Empirical method

This method takes in consideration that RFID antennas usually operates near their resonance frequency. Thus, the higher order resonant modes may be neglected [9]. The equivalent circuit of the helical antenna's input impedance is composed of five lumped passive elements, as presented Fig. 3.

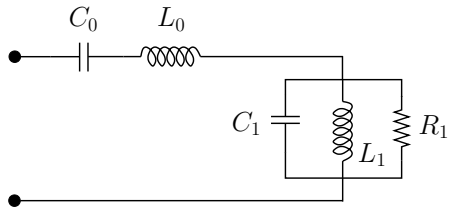


Fig. 3. Equivalent circuit of the helical antenna operating near their first resonance

The derivation of the different elements uses a graphical method initially in order to extract the first and the second resonance frequencies $f_{01}$ and $f_{02}$. At these frequencies, the imaginary part vanishes and the real parts are equal to $R_{0L}$ and $R_{1L}$ respectively. The capacitance $C_{0L}$ is determined using the reactance $X_{LF}$ of the helical antenna at a frequency $f_{LF} \ll f_{01}$ well below the antenna's first resonance frequency:

$$C_{0L} = \frac{1}{2\pi f_{LF} \left| X_{LF} \right|} \tag{3}$$

The inductance $L_{0L}$ is selected in order to resonate with $C_{0L}$ at the second resonant frequency $f_{02}$:

$$L_{0L} = \frac{1}{{\omega_{02}}^2 C_{0L}} \tag{4}$$

Moreover, the values of $R_{1L}$, $L_{1L}$, $C_{1L}$ are determined by the equations in (5) such way to obtain the first resonance $f_{01}$.

$$\begin{cases} R_{1L} = \dfrac{{R_{0L}}^2 + A^2}{A} \\ L_{1L} = \dfrac{{R_{0L}}^2 + A^2}{A} \cdot \left( \dfrac{\omega_{01}}{{\omega_{02}}^2} - \dfrac{1}{\omega_{02}} \right) \\ C_{1L} = \dfrac{A}{{R_{0L}}^2 + A^2} \cdot \left( \dfrac{1}{{\omega_{01}}^2 - {\omega_{02}}^2} \right) \end{cases} \tag{5}$$

The terms $\omega_{01} = 2\pi f_{01}$ and $\omega_{02} = 2\pi f_{02}$ are the first and the second resonant pulsations. The term $A$ is depending on the wire dipole antenna's input resistance $R_{0L} = 73\ \Omega$ :

$$A = -\sqrt{R_{1L} R_{0L} - {R_{0L}}^2} \tag{6}$$

### *B. Rational approximation of the antenna's input impedance*

The vector fitting (VFIT) algorithm is able to give the rational approximation of a network's frequency response by a set of stable poles [10]. This method was initially employed for the electrical power distribution systems or high power transformers and was extended to higher frequency especially in microwave as for example to model the characteristics of ultra wide-band antennas such as their input impedance or transfer function. [11].

For the helical antenna's case, the rational approximation of the input admittance $Y(j\omega)$, can be written as in the following equation:

$$Y(\jmath\omega) \approx Y_{fit}(\jmath\omega) = \sum_{m=1}^{N} \frac{c_m}{\jmath\omega - a_m} + d + \jmath\omega \cdot e \tag{7}$$

where $\omega = 2\pi f$, $f$ being the frequency. The terms $c_m$ and $a_m$ are the residues and the poles respectively, which may be real or complex conjugate. The terms $d$ and $e$ are real ones.

By using this approximation, the equivalent electrical circuit modeling the antenna's behavior is the one depicted in Fig. 4.

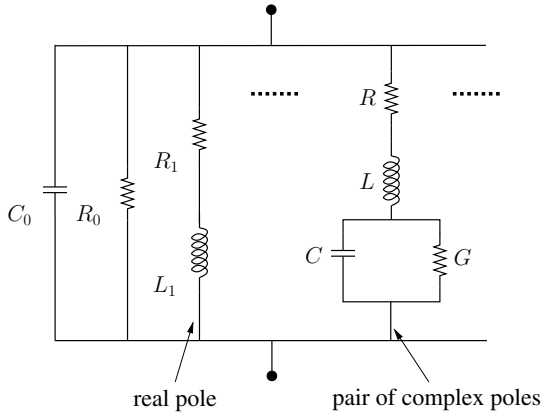


Fig. 4. Equivalent electrical circuit extracted by using "vector fitting" algorithm

Here, $C_0 = e$ and $R_0 = \dfrac{1}{d}$. Each real pole $a_m$ and its corresponding residue $c_m$ gives an **RL**-branch in the equivalent circuit with:

$$\begin{cases} R_1 = -\dfrac{a_m}{c_m} \\ L_1 = \dfrac{1}{c_m} \end{cases} \tag{8}$$

Each complex conjugate pole $a_m = {a_m}' + \jmath \cdot {a_m}''$ and its corresponding residue: $c_m = {c_m}' + \jmath \cdot {c_m}''$ gives an **RLCG**-branch with:

$$\begin{cases} R = \left(-2{a_m}' + 2\left({c_m}'{a_m}' + {c_m}''{a_m}''\right) L\right) L \\ L = \dfrac{1}{2{c_m}'} \\ C = \dfrac{1}{\left({{a_m}'}^2 + {{a_m}''}^2 + 2\left({c_m}'{a_m}' + {c_m}''{a_m}''\right) R\right) L} \\ G = -2\left({c_m}'{a_m}' + {c_m}''{a_m}''\right) LC \end{cases} \tag{9}$$

### *C. Simulation results*

The antenna's input impedance obtained from electromagnetic simulation (CST) was employed in order to extract the models (graphical and VFIT methods). Then, circuit simulations performed by using Keysight's ADS© software, are giving the impedance presented in Fig. 5 (for the real part) and Fig. 6 (for the imaginary part).

With the empirical approach, the model, composed by only five lumped elements, is presented in Table III. The VFIT model has eight complex conjugate poles, which corresponds to 18 elements. Some of the resistors are negative despite the fact that the model is passive (poles with negative real part).

The obtained poles are the following: $(-2.43+\jmath\cdot0.67)\cdot10^9$; $(-2.43-\jmath\cdot0.67)\cdot10^9$; $(-0.19+\jmath\cdot5.41)\cdot10^9$; $(-0.19-\jmath\cdot5.41)\cdot10^9$; $(-0.15+\jmath\cdot044)\cdot10^9$; $(-0.15-\jmath\cdot16.044)\cdot10^9$; $(-6.5+\jmath\cdot34.42)\cdot10^9$ and $(-6.5-\jmath\cdot34.42)\cdot10^9$.

TABLE III
EMPIRICAL MODEL'S LUMPED COMPONENTS

| $\mathbf{C_{0L}}$ [pF] | $\mathbf{L_{0L}}$ [nH] | $\mathbf{C_{1L}}$ [pF] | $\mathbf{L_{1L}}$ [nH] | $\mathbf{R_{1L}}[\Omega]$ |
|---|---|---|---|---|
| 0.53 | 21.3 | 0.27 | 41.83 | 2.88 |

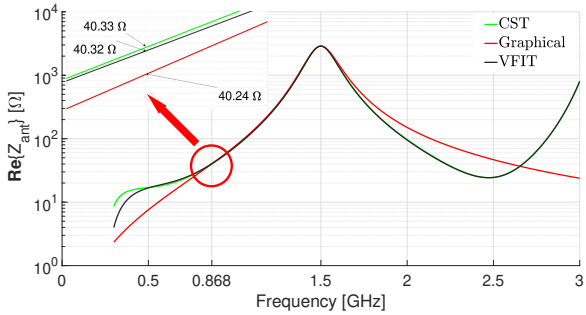


Fig. 5. Resistance of the designed antenna (CST), of the VFIT model and of the model extracted by the graphical method.

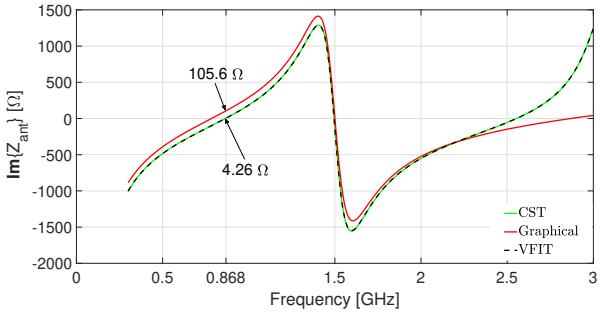


Fig. 6. Reactance of the designed antenna (CST), of the VFIT model and of the model extracted by the graphical method.

From the results presented in Fig. 5 and Fig. 6, one can remark that at the resonance frequency (i.e., 868 MHz), the input impedance of the two models are closed to the designed antenna's input impedance. Moreover, the two models are accurate at low frequencies.

As the empirical model is extracted from the antenna behavior, its main advantage is that one can identify which specific element in the model will vary when the corresponding antenna's physical parameter is varying. However, the proposed model extraction method cannot be extrapolated to other antenna topology.

VFIT gives the most precise model for the simulated frequency range. However, the obtained model is more complex which is a low constraint regarding nowadays computational capabilities. Moreover, the VFIT model extraction method is independent on the antenna shape and can be used with good precision for any antenna geometry, even for multi-band antennas. The main drawback is that the obtained model is independent on the antenna's physical dimensions.

Consequently, both methods are giving an exploitable model at the resonance frequency and, depending on the future usage, one of the methods may be employed.

## IV. Conclusion

This paper focused on the model of a helical antenna designed for RFID yarn in the context of wearable electronics. Firstly, the paper presented the antenna's design and studied the variation of the antenna's electric parameters with respect of stretching, which is inevitable in the context the proposed application. Secondly, two methods to extract equivalent electric models of the input impedance have been presented and applied. More specifically, an empirical method taking into account the antenna geometry and physics was compared with a more general method based on poles-residues identification. The two methods were compared in terms of complexity, accuracy and respect of the antenna's behavior. Future work will be dedicated to identify a more accurate empirical model and to verify which is the element in the model varying with respect of antenna's geometry variation.

## Acknowledgment

This work has been supported by "La Région Auvergne Rhône-Alpes" Lyon, France and with the collaboration of Primo1D company.

## References

[1] D. Evans, "The Internet of Things. How the next evolution of the Internet is changing everything," Apr. 2011.
[2] L. Davoli, L. Belli, A. Cilfone, and G. Ferrari, "From micro to macro IoT: Challenges and solutions in the integration of IEEE 802.15.4/802.11 and sub-GHz technologies," *IEEE Internet of Things Journal*, vol. 5, no. 2, pp. 784–793, Apr. 2018.
[3] S. Al-Sarawi, M. Anbar, K. Alieyan, and M. Alzubaidi, "Internet of things (IoT) communication protocols: Review," in *8th International Conference on Information Technology (ICIT)*, May 2017, pp. 685–690.
[4] S. Tedjini, G. Andia-Vera, M. Zurita, R. C. S. Freire, and Y. Duroc, "Augmented RFID tags," in *IEEE Topical Conf. Wireless Sensors and Sensor Networks (WiSNet)*, Jan. 2016, pp. 67–70.
[5] Y. Duroc and S. Tedjini, "RFID: a key technology for humanity," *Comptes Rendus Physique - Comptes Rendus de l'Académie des Sciences*, vol. 19, no. 1-2, pp. 64–71, Feb. 2018.
[6] P. V. Nikitin and K. V. S. Rao, "Antennas and propagation in UHF RFID systems," in *IEEE Int. Conf. RFID*, Apr. 2008, pp. 277–288.
[7] G. Andía, "Slenderly and conformable passive UHF RFID yarn," in *IEEE International Conference on RFID (RFID)*, May 2017, pp. 130–136.
[8] S. Benouakta, S. Koley, F. Hutu, and Y. Duroc, "Conception d'une antenne hélice pour fil textile RFID UHF extensible," in *Journées Nationales Micro-Ondes, France - in press.*, May 2019.
[9] Y. Liao, K. Cai, T. H. Hubing, and X. Wang, "Equivalent circuit of normal mode helical antennas using frequency-independent lumped elements," *IEEE Transactions on Antennas and Propagation*, vol. 62, no. 11, pp. 5885–5888, Nov. 2014.
[10] B. Gustavsen and A. Semlyen, "Rational approximation of frequency domain responses by vector fitting," *IEEE Transactions on Power Delivery*, vol. 14, no. 3, pp. 1052–1061, Jul. 1999.
[11] Y. Duroc, A. Ghiotto, T. P. Vuong, and S. Tedjini, "Parametric modeling of ultrawideband antennas," *IEEE Transactions on Antennas and Propagation*, vol. 55, no. 11, pp. 3103–3105, Nov. 2007.